Pawpaw (Asimina triloba L.) ramet leaf-area scaling and patch foliar estimation in a midwestern upland forest1

Author: Sipe, Timothy W.

Source: The Journal of the Torrey Botanical Society, 150(2) : 282-295

Published By: Torrey Botanical Society

URL: https://doi.org/10.3159/TORREY-D-22-00009.1

Journal of the Torrey Botanical Society 150(2): 282–295, 2023.

Pawpaw (*Asimina triloba* L.) ramet leaf-area scaling and patch foliar estimation in a midwestern upland forest[1]

Timothy W. Sipe[2]
Department of Biology, Franklin & Marshall College, Lancaster, PA 17604

Abstract. Forest understory shrub and small tree taxa vary in their shoot architectures in response to their physical and biotic environments and in turn alter the conditions around them, particularly patterns of light. Clonal shrubs establish patches that expand three dimensionally over time as new ramets are produced and the ramet population responds to environmental heterogeneity, competition, and disturbance. Ramet leaf-area scaling and patch foliar structure were examined for the shade-tolerant clonal species *Asimina triloba* L. Dunal (pawpaw) on upland sites in a mixed-deciduous, old-growth forest preserve in west-central Indiana, USA to address three questions: (a) How strong are predictive relationships for ramet foliar organization across individual leaves, leaf clusters, and whole ramets of differing size? (b) Is it possible to estimate patch foliar area nondestructively and accurately using scaling factors derived from the analysis of ramet foliar organization? (c) How does foliar structure differ within and across patches, including total leaf area estimated with scaling factors? A sample of 48 ramets spanning a wide size range of 0.25 to 2.5 m in height was extracted from the field and analyzed for whole-ramet relationships between main-stem length and several foliar variables. Forty-one long and short leaf clusters from these ramets were used to quantify relationships among cluster size, individual leaf area, and total leaf area and to estimate total ramet leaf area. Eight patches varying in areal size, stature, and ramet density were measured for numerous structural variables and a single cluster-based scaling factor was used to estimate total leaf area, leaf-area index (LAI), and leaf-area density in 2×2 m quadrats along continuous transects through patches. The results showed strong curve fits among foliar variables for both the ramet-level and cluster-level relationships and suggest that leaf clusters may be an important focus of foliar organization and dynamic adjustment for *A. triloba*. The eight patches showed substantial within-patch structural variation and their means differed significantly for all structural variables including LAI, which ranged from 0.42 to 1.28 m^2 m^{-2}. The results also suggest that total leaf area for *A. triloba* patches in undisturbed, mature upland forests like those in this study may be estimated nondestructively by counting the number of clusters projected over a sample plot base and multiplying by a weighted mean total cluster leaf area derived from the cluster-scaling relationships. This promising method should be tested across other physiographic conditions and forest types and where nontrivial canopy disturbance has affected *A. triloba* patch history.

Key words: clonal shrub, forest understory, plant architecture

Extensive research has been done on the detailed architecture of woody plants to understand structure–function relationships at many scales and to probe fundamental questions regarding developmental, biomechanical, and physiological correlates of different architectural designs along with their ecological significance (Küppers 1989; Pearcy *et al.* 2005). The majority of the ecological research in mesic forests has been on the interplay between architecture and light, particularly how architecture influences the efficiency of light capture for photosynthesis (e.g., Kempf and Pickett 1981; Nicola and Pickett 1983; Pearcy and Yang 1996; Luken *et al.* 1997; Kawamura and Takeda 2004). The spatial–temporal complexity of photosynthetic photon flux density (PPFD) patterns in closed-canopy communities challenges plants to produce effective foliar displays and opens the door to a wide array of solutions involving the interplay between architecture and physiology (Kawamura and Takeda 2002; Sterck *et al.* 2013). Plant architecture in turn affects microenvironments within a plant's sphere of influence.

Shade-tolerant understory shrub and small tree taxa differ inherently in their stature, stem architecture, and clonality and in their phenotypic flexibility in response to local environments (Pickett and Kempf 1980; Valladares *et al.* 2000; Iwabe *et al.* 2021). These variables yield a structural spectrum within and across species that has varying consequences for the surrounding community. The impacts of clonal understory

[1] Financial support for summer research students was provided by Wabash College and Franklin & Marshall College. The Biology Department at Wabash generously provided laboratory space, a vehicle for transportation to the field site, and other support. Students Nicholas Boyce and Sara Lobdell contributed significantly to the fieldwork and data entry for this project.

[2] Author for correspondence: tsipe@fandm.edu.

doi: 10.3159/TORREY-D-22-00009.1

Received for publication April 7, 2022, and in revised form October 23, 2022; first published December 28, 2022.

shrubs may grow over time as genets establish, ramets multiply internally and on the margins, and overall patch structure increasingly dominates an area. Multiple genets may coalesce and form a continuous stratum across a large expanse, particularly on sites best suited to the species' resource requirements.

Asimina triloba L. Dunal (pawpaw) is a native deciduous understory shrub/small tree that establishes clonal patches in temperate forests across its broad range in the eastern USA. Published research on *A. triloba* biology and ecology other than arboriculture includes patch genotypic composition (Botkins *et al*. 2012), pollination ecology (Willson and Schemske 1980), ecophysiology (Young 1985, 1987; Young and Yavitt 1987; Jacquart *et al*. 1992; Nash and Graves 1993; Augspurger *et al*. 2005), ramet demography, growth and clonal persistence (Hosaka *et al*. 2005, 2008), geographic variation in ramet size and reproduction (Lagrange and Tramer 1985), patch responses to ramet damage (Hosaka *et al*. 2016), herbivore impacts on patch condition after invasive shrub removal (Mercader *et al*. 2020), twig biomechanics in relation to storm wind damage potential (Goodrich *et al*. 2016), effects of chronic deer browsing on *A. triloba* abundance (McGarvey *et al*. 2013; Slater and Anderson 2014), and correlations with tree seedling abundance and survival (Baumer and Runkle 2010). Curiously—given its distinctive growth form compared with other eastern North American shrub taxa—there are no published studies of *A. triloba*'s architectural relationships under forested conditions except for Young (1985), who described crown height, branching, and leaf display contrasts between *A. triloba* and a co-occurring evergreen shrub (*Ilex opaca* Ait., American holly) in a *Carya–Quercus* forest in east-central Virginia, USA.

Quantifying shoot architecture and clonal patch structure can improve our understanding of shrub impacts on understory light environments, particularly if leaf-area scaling follows consistent patterns. These issues are relevant to ongoing research on forest composition, light regimes, and regeneration patterns at Allee Memorial Woods (AMW), an old-growth preserve in west-central Indiana. *Asimina triloba* is the most distinctive component of the shrub stratum at AMW, with patches of varying three-dimensional size and ramet density occurring across the upland portions of the preserve in addition to its presence on lower slopes and ravine bottoms. Maximum ramet heights and diameters at AMW are generally in a transition zone between shrub and small tree classes. They are larger than the ramets measured by Hosaka *et al*. (2008), comparable with those sampled by Young (1985), and smaller than the tree-sized stems analyzed by Lagrange and Tramer (1985).

Our initial understory PPFD measurements at AMW did not include sampling in *A. triloba* patches (Sipe and Yamulla 2021), but we have since measured PPFD attenuation by *A. triloba* intensively in the lower 3 m. We were interested in the relationship between PPFD transmission and *A. triloba* leaf area, especially leaf-area index (LAI, total leaf area per unit ground area) and leaf-area density (LAD, total leaf area per unit canopy volume), so an important part of this effort has focused on determining whether rapid, nondestructive estimates of patch foliage could be acquired using leaf-area scaling relationships.

Several methods for estimating LAI have been developed to date that differ in their measurement requirements, assumptions, accuracy, and trade-offs (Fassnacht *et al*. 1994; Weiss et al. 2004). Direct methods involve physically measuring leaf area, either live foliage or litter, and are considered to be the most accurate, but they require the most time and effort. Indirect methods, including canopy imaging or back-calculating LAI from measurements of light extinction through a vertical profile, are faster but less accurate unless calibrated against direct measurements. The leaf cluster scaling approach explored in this study represents an intermediate strategy along the spectrum of LAI determination methods. Total foliar area and LAI are derived not by direct measurements of live or dead leaves, but they are based explicitly on quantified leaf area, in contrast to the indirect methods. The results are reported in this paper along with underlying patterns of ramet foliar structure.

The focus of this study is not on theoretical considerations of woody shoot architecture, and thus does not involve the kinds of detailed measurements of stem branching patterns, leaf sizes, positions and orientations, and crown dimensions quantified in other research (e.g., Pearcy *et al*. 2005; Laurans and Vincent 2016). The term "architecture" is therefore used in a more general sense throughout this paper. Similarly, the

dynamics of clonal establishment, expansion, ramet demography, and response to spatial environmental heterogeneity are critical processes of clonal plant ecology (Wang *et al*. 2020), and they ultimately influence *A. triloba* patch structure, LAI, and PPFD transmission. However, the research reported here does not test hypotheses about the regulation of ramet design, density, growth, or whole-clone integration and performance.

The central questions of this study were as follows: (a) How strong are predictive relationships for ramet foliar organization across individual leaves, leaf clusters, and whole ramets of differing size? (b) Is it possible to estimate patch foliar area nondestructively and accurately using scaling factors derived from the analysis of ramet foliar organization? (c) How does foliar structure, including total leaf area estimated with scaling factors, differ within and across patches?

Materials and Methods. STUDY SPECIES. *Asimina triloba* prefers moist but well-drained fertile soils in bottomlands but also occurs in mesic upland forests. It is shade tolerant but grows fastest under enhanced light associated with canopy disturbance, especially small to medium-sized canopy gaps (Hosaka *et al*. 2008). Flowering and fruiting occur only after a size threshold has been reached (Willson and Schemske 1980), which occurs more often under higher light (Hosaka *et al*. 2008).

Patch expansion through new ramet production usually begins not long after establishment of a genet through seed germination. Ramet density also increases within the clone interior over time, solidifying *A. triloba*'s dominance within the patch footprint (Hosaka *et al*. 2005). Connections between ramets are maintained for at least several years. Ramets can reach 10 m in height and live for at least 30 years. Once established, the patches tend to remain fairly persistent even though ramets may turn over (Hosaka *et al*. 2008). Patch symmetry varies in forest understories as ramet density, height, foliar area, and horizontal patch extension rates respond to localized variation in resource availability, disturbance-related damage, or ramet mortality. Neighboring patches may meet and grade into one another, blurring their original boundaries.

The obovate laminas of *A. triloba*'s simple leaves are unusually large, up to 13 cm wide and 30 cm long, compared with the individual undivided leaves or compound leaflets of most woody species in eastern North American forests. They appear in clusters of 2–11 leaves each on terminal portions of first-order (main stem) and long second-order branch axes, and also on distinctively shorter (typically < 50 cm) second- and third-order branches diverging from the main stem and second-order branches, respectively. Foliage on the main stem and longer second-order branch axes will be referred to hereafter as "long clusters" of leaves, whereas foliage on the shorter branch segments will be referred to as "short clusters." The term "cluster size" will be used to represent the number of leaves in a cluster, regardless of whether it is a long cluster or a short cluster.

Asimina triloba foliage is strongly plagiotropic in shaded, undisturbed conditions (Young 1985). The main stem and longer second-order branches arch over to become nearly horizontal and the long cluster leaves on them are arrayed in a linear alternating series with more widely spaced internodes and minimal overlap among leaves. The short-cluster branches have shorter internodes and the leaves are displayed mostly horizontally in a manner resembling a whorled compound leaf with little self shading.

STUDY SITE. Allee Memorial Woods is an 80-ha preserved site containing old-growth areas (*sensu* Parker 1989) that are among the best remnants of the original deciduous forests of Indiana, USA (Lindsey *et al*. 1969). The study site (39.863°N, 87.280°W) is located near the boundary of the central hardwoods and forest–prairie ecoregions in the central glacial till plain of Indiana. The preserve is on dissected sandstone-capped topography bordering a river, with steep-walled gorges up to 40 m deep that divide the preserve into three main upland peninsulas where the *A. triloba* patches in this study were located (Petty 1964). The soils are derived from a thin mantle of postglacial loess and granitic till overlying sandstone and vary from silt loams on the upland peninsulas to nutrient-poor sandy loams on the eroded gorge margins. Soil pH averages 5.0 (range 4.3–7.2), with highest values in ravines and gorges, and the upland soils are well drained (Petty *et al*. 1961). Climate data measured across 1991–2020 at the nearest U.S. National Weather Service station 46 km to the south with an elevation comparable with AMW show a mean

annual temperature of 19.7 °C (monthly range 4.4–32.4 °C) and mean total annual precipitation of 113.5 cm (monthly range 6.3–12.9 cm).

Much of AMW was affected by selective cutting during 1890–1920, but a section of uncut forest dominated by *Fagus grandifolia* L. (American beech) and *Acer saccharum* L. (sugar maple) survived intact. No forest management or other direct human impacts have occurred in the older stands since about 1920. Fire occurred in the region before European settlement in the early 1800s, but there are no records or evidence of fire in the vicinity of AMW since then. Measurements of dead snags, fallen trees, and coarse woody debris in 2014 suggest that the preserve has not experienced large-magnitude disturbance since the logging era.

Forest structure and composition were mapped and measured during 2011–12 in permanent grids within three stands that were used in this study (Sipe and Yamulla 2021). The stands are less than 500 m apart in similar physiographic positions. Stand A (1.2 ha) is a comparatively level *Quercus*-dominated site that was heavily cut before 1925. Stand B (2.05 ha) is the uncut area and was considered to be an old-growth *F. grandifolia–Ac. saccharum* forest as of 1960. Stand C (3.2 ha) has a mixed overstory composition and disturbance history, with some records and evidence of selective cutting across approximately half of the stand before 1915.

All stands exhibited pronounced compositional divergence across strata as of 2011–12. The overstories are dominated by varying proportions of *Liriodendron tulipifera* L.(tulip poplar), *Quercus alba* L. (white oak), *Quercus rubra* L. (northern red oak), *Quercus velutina* Lam. (black oak), and some *Ac. saccharum* L. (sugar maple) and *F. grandifolia* Ehrh. (American beech). Both the mid-sized (7.6–50.7 cm diameter at breast height [DBH]) and sapling (1 m tall to 7.6 cm DBH, hereafter 1 m–7.6 cm) strata are dominated by *Ac. saccharum* and *F. grandifolia* (Sipe and Yamulla 2021). Two other shrub species occur with varying frequency across the preserve, *Lindera benzoin* L. (spicebush) and *Dirca palustris* L. (leatherwood). The herbaceous community is diverse and dense on the gorge slopes and bottoms, but it is considerably reduced across the uplands. Invasive herb and shrub species are relatively uncommon, especially in the upland stands.

Ramet Architecture. Sets of 9–10 undamaged ramets were randomly selected within each of five main-stem height classes (0–0.49, 0.50–0.99, 1.0–1.49, 1.5–1.99, and 2.0–2.5 m) from three *A. triloba* patches in Stand B that were representative of the upland patches across AMW. The ramets were cut at the base and taken to the lab, where main-stem length was measured to the terminal bud on the longest stem axis and basal diameter was measured to the nearest 0.1 mm 2.5 cm above the cut base. The numbers of long clusters and short clusters were counted, along with the number of leaves in each cluster and total number of leaves per ramet, for overall sample sizes of 48 ramets, 609 clusters (378 long, 231 short), and 3,142 leaves.

Scatterplots and regressions (linear, quadratic, exponential) were calculated for numerous relationships among these variables, including (a) main-stem length *versus* basal diameter, (b) number of long, short, and combined leaf clusters *versus* main-stem length, (c) number of short clusters *versus* number of long clusters, (d) total number of long-cluster leaves *versus* total number of short-cluster leaves, (e) total number of leaves *versus* total number of clusters per ramet, and (f) total number of leaves *versus* main-stem length. Frequency distributions of clusters with different numbers of leaves were also generated, and chi-square was used to test for the difference between long and short clusters in their distributions.

Cluster and Ramet Leaf Area. It was not possible to measure leaf area for all leaf clusters when the ramets were processed. Therefore a total of 41 leaf clusters was selected from the 48 ramets to provide data on cluster foliar structure and for estimating total ramet leaf areas using cluster-based scaling. The clusters were randomly selected within different combinations of cluster type (long *versus* short) and cluster size (number of leaves). They included (a) 24 long clusters, ranging from 3 to 10 leaves per cluster, with 2–4 clusters in each leaf number category, totaling 155 leaves; and (b) 17 short clusters, ranging from 1 to 6 leaves per cluster, with 2–3 clusters per category, totaling 57 leaves. All leaves were pressed and oven-dried, and the area of each leaf was measured to the nearest 1 mm^2 with an area meter (LI-3100, Li-Cor, Inc., Lincoln, NE).

Total leaf area was summed for each cluster and descriptive statistics were produced for total cluster leaf area represented by each combination of

cluster size and number of leaves. Total cluster leaf area was plotted against number of leaves per cluster for long clusters, for short clusters, and for combined clusters, and regression relationships were determined for these plots.

In addition, two analyses were done to determine whether mean leaf area varied systematically within clusters or across clusters of different size. First, mean leaf area was calculated for successive leaf positions (leaf order, oldest to youngest during leaf expansion) across all clusters of the same size. This was done for all cluster sizes; mean leaf area per position was plotted against cluster size and a linear regression was fit to the plot. This process was done separately for long and short clusters. Second, the mean total cluster leaf area was calculated for each cluster size and plotted against cluster size for long clusters, for short clusters, and for all clusters combined. Regressions were fit to all three scatterplots.

Total leaf area was then estimated for each of the 48 ramets by multiplying the number of leaf clusters of each size by the mean leaf area for that size and summing the products across all cluster sizes. This was done separately for long and short clusters on the ramet and the totals were then summed to yield total ramet leaf area. Estimated total ramet leaf area was plotted against ramet main-stem length and a regression was fit to the scatterplot.

CLUSTER GROUP LEAF AREA ESTIMATION. Estimating total *A. triloba* foliage nondestructively in the field can be done successfully if the ramet-level and cluster-level relationships just described are sufficiently predictive. In principle, it would be possible to record selected information about every ramet within a defined sample area and apply a ramet-level scaling factor—for example, total estimated leaf area *versus* main-stem length—and then sum the area across all ramets. However, leaves or leaf clusters projected over a horizontal sample plot may be attached to ramets rooted outside the plot, and leaves/clusters projected outside the plot could be attached to ramets rooted inside the area. Thus ramet-based scaling would introduce variable error in the estimation of total leaf area projected over the plot where the foliage most influential for affecting light attenuation is located. This "displacement" error is likely to be more consequential for species like *A. triloba*, in which comparatively fewer larger leaves are arrayed as clusters on long main stems and branches that are strongly plagiotropic and extend laterally for sizable distances relative to main-stem height. In addition, ramet populations in the field include damaged and recovering individuals that may not show the same overall main-stem/branching patterns and foliar scaling relationships as the undamaged ramets measured in this study.

A different strategy would be to count the total number of leaf clusters projected vertically over a plot and scale directly to total plot leaf area using conversions based on mean cluster leaf area rather than ramet leaf area. This would be analogous to the common procedure of measuring plant cover projected over a defined plot without reference to whether foliage is on a plant rooted inside or outside the plot.

The key to this approach is identifying the best mean cluster leaf area to use as the multiplier against the number of clusters recorded in a plot. The mean cluster leaf area calculated across the 41 measured clusters (575 cm^2) is not likely to be the best multiplier for two reasons. First, the cluster sample was not fully random but stratified—clusters were randomly selected for each of eight long cluster sizes and six short cluster sizes to be sure the entire size range was included—and as such may not represent the proportions of long and short cluster sizes that occur in the field. Second, the calculated mean leaf area across all clusters masks a 3.5-fold difference between the mean leaf areas for the long and short clusters (817 *versus* 233 cm^2).

A two-step weighting procedure was used to generate a more representative multiplier for estimating the total leaf area of any group of clusters. The first weighting step was done separately for long and short clusters by (a) calculating mean total leaf area for each cluster size, (b) determining the proportions of all recorded clusters represented by each cluster size, (c) multiplying the mean cluster size leaf area by the proportion for each cluster size, and (d) summing these products. This procedure generated a separate single-weighted mean leaf area for long (763 cm^2) and short (147 cm^2) clusters. The second weighting step involved converting the two single-weighted cluster leaf areas into a combined cluster leaf area. The ratio of long ($N = 378$) to short ($N = 231$) clusters recorded across the 48 ramets was 61:39. These proportions were multiplied by the corresponding single-weighted mean leaf areas for

Table 1. Results of ramet-level and leaf cluster-level regressions. Equations and coefficients are as follows: (a) linear, $Y = aX + Y_0$; (b) quadratic, $Y = aX + bX^2 + Y_0$; (c) exponential, $Y = a(e^{bx})$. All three equations were fit to every scatterplot and results for the regression equation with the highest coefficient of determination (R^2) are shown for each pair of variables.

X	*Y*	Equation	*N*	*P*	R^2	Y_0	*a*	*b*
Ramet-level relationships								
Stem length	Basal diameter	Linear	48	< 0.0001	0.947	set to 0	1.057	—
Stem length	No. long clusters	Exponential	48	< 0.0001	0.736	—	1.143	1.253
Stem length	No. short clusters	Exponential	48	< 0.0001	0.549	—	0.327	1.651
Stem length	Total no. clusters	Exponential	48	< 0.0001	0.681	—	1.412	1.395
Stem length	Total no. leaves	Exponential	48	< 0.0001	0.735	—	9.438	1.258
Stem length	Total leaf area	Exponential	48	< 0.0001	0.760	—	0.127	1.138
No. long clusters	No. short clusters	Linear	48	< 0.0001	0.788	−1.29	0.776	—
No. long cluster leaves	No. short cluster leaves	Linear	48	< 0.0001	0.793	−4.67	0.453	—
Total no. clusters	Total no. leaves	Linear	48	< 0.0001	0.978	set to 0	4.808	—
Cluster-level relationships								
No. leaves, long clusters	Long cluster leaf area	Linear	24	< 0.0001	0.900	−380.29	185.39	—
No. leaves, short clusters	Short cluster leaf area	Quadratic	17	< 0.0001	0.935	9.63	14.74	12.465
No. leaves, combined clusters	Combined cluster leaf area	Quadratic	41	< 0.0001	0.928	−70.75	59.03	10.275
Leaf position on long clusters	Mean leaf area	Linear	8	0.001	0.853	42.3	11.67	—
Leaf position on short clusters	Mean leaf area	Linear	6	0.001	0.947	23.1	11.24	—

the long and short clusters to generate a double-weighted combined cluster multiplier (523 cm^2).

Patch Foliar Structure. Stands A, B, and C were explored before ramet extraction to identify all distinctive *A. triloba* patches that were located within or near the permanent study grids. Eight well-defined patches differing in patch areal size, apparent ramet and foliar densities, and canopy height were selected for study in undisturbed upland locations. A 2-m-wide belt transect was positioned through the center of each patch along the long axis, and the transect was divided into contiguous 2 × 2 m quadrats placed 0–2 m, 2–4 m, 4–6 m, *etc*. on either side of the patch midpoint. Within each quadrat, the total number of *A. triloba* stems was counted, the minimum and maximum foliar heights were measured, canopy depth was calculated (difference between maximum and minimum foliar heights), and the total number of leaf clusters was counted without distinguishing long *versus* short clusters.

Total leaf area (m^2) per quadrat was estimated by multiplying the total number of clusters by the double-weighted combined cluster scaling factor (523 cm^2 per cluster). Leaf area index ($m^2\ m^{-2}$) per quadrat was then calculated by dividing total leaf area by 4 and leaf area density ($m^2\ m^{-3}$) was calculated by dividing total leaf area by canopy volume (= canopy depth × 4).

Differences in means among the eight patches were tested for each structural variable using either parametric one-way ANOVA with Tukey pairwise comparisons (number of *A. triloba* stems, maximum height, minimum height, canopy depth) or nonparametric Kruskal–Wallis one-way ANOVA with Dunn's pairwise tests (all other variables). Each variable was also plotted against patch size (transect length) and regressions were fit to see if patch ramet density or foliar structure changed predictably with size.

Results. Ramet Architecture. Numerous strong relationships occurred among variables at both the whole-ramet level and at the leaf-cluster level (Table 1). Ramet main stems showed a very strong linear relationship between basal diameter and length (Fig. 1f). The total number of leaf clusters per ramet ranged from 1 to 65 (mean 12.7, SD 15.3). The numbers of long clusters and short clusters were both related exponentially to main-stem length (Table 1, Fig. 1a). There were 65% more long clusters on average (mean 7.9, range 2–11) than short clusters (mean 4.8, range 0–7), and their medians (4.5 and 2.0, respectively) differed significantly (Mann-Whitney U = 774.5, P = 0.005). The parallel nature of the long- and

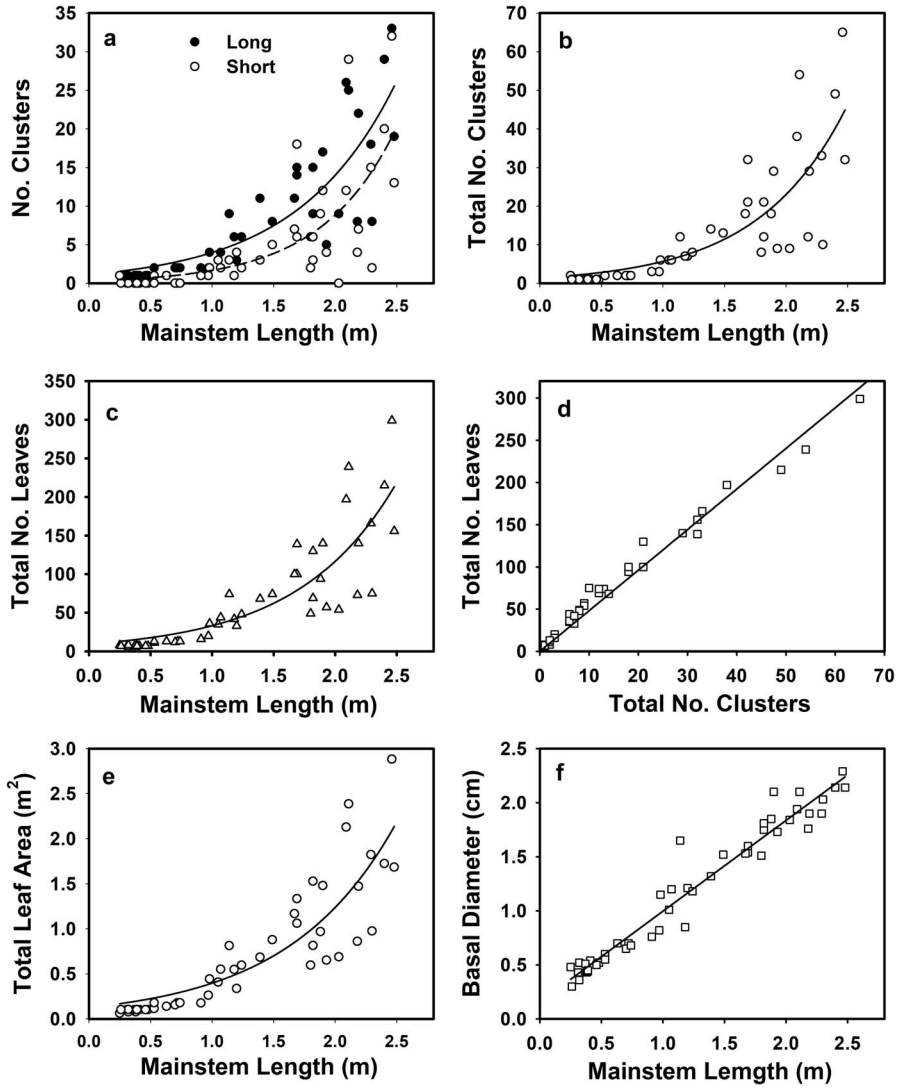

FIG. 1. Size-related relationships for 48 *Asimina triloba* ramets, including (a) number of long and short leaf clusters, (b) total number of leaf clusters, (c) total number of leaves, (e) estimated total ramet leaf area, and (f) basal stem diameter *versus* main-stem length, plus (d) total number of leaves *versus* total number of clusters per ramet. Exponential curves fit better than quadratic curves for scatterplots a–c and e, whereas linear regressions were the best fit for scatterplots d and f. Equations: linear, $Y = a(X) + Y_0$; exponential, $Y = a(e^{bx})$.

short-cluster curves produced a similar exponential relationship between the total number of clusters and main-stem length (Table 1, Fig. 1b), and there were highly significant linear correlations between both the numbers of long clusters and short clusters per ramet and the numbers of long-cluster leaves and short-cluster leaves per ramet (Table 1).

The frequency distributions of cluster size (number of leaves) differed significantly between the long and short clusters ($\chi^2 = 533.0$, $P < 0.001$, d.f. = 20; Fig. 2). Long clusters averaged 64% more leaves (mean 6.56, range 5.0–9.0) than short clusters (mean 3.99, range 2.8–5.5), and their medians (6.5 and 4.0, respectively) differed significantly (Mann-Whitney U = 9.00, $P < 0.001$). Ramets thus had 2.8-fold more total leaves in long clusters (mean 48.3, range 5–185) than in short clusters (mean 17.2, range 0–114), and their medians (37.5 and 9.0, respectively) differed significantly (Mann-Whitney U = 590.0, $P < 0.001$). The total number of leaves per ramet ranged from 6 to 299 (mean 65.5, SD 70.5) and

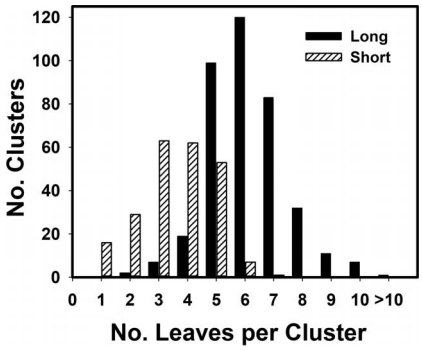

FIG. 2. Frequency distributions of long ($N = 378$, mean = 6.6) and short ($N = 231$, mean = 4.0) clusters with differing number of leaves per cluster across 48 ramets.

was strongly and linearly correlated with the total number of clusters per ramet (Table 1, Fig. 1d), despite the differences in long- *versus* short-cluster contributions to total ramet foliage.

CLUSTER AND RAMET LEAF AREA. Mean leaf area generally rose to a peak and then declined somewhat as a function of leaf position within clusters, and the trend became more pronounced with cluster size (Fig. 3a). The shape of the relationship was broadly similar across cluster sizes, but larger clusters had greater mean leaf areas overall, especially for younger leaves. There were strong linear relationships between mean leaf area and the number of leaves per cluster (Table 1, Fig. 3b). The slopes were very similar for the long- and short-cluster regressions, but long clusters showed greater mean leaf areas for all leaf positions.

This pattern was reinforced by comparing individual leaf areas and total cluster leaf areas directly between the two cluster types (Table 2). Mean individual leaf area was greater by 80% on long clusters than short clusters (Mann-Whitney U = 1,702.5, $P < 0.001$), and total cluster leaf area

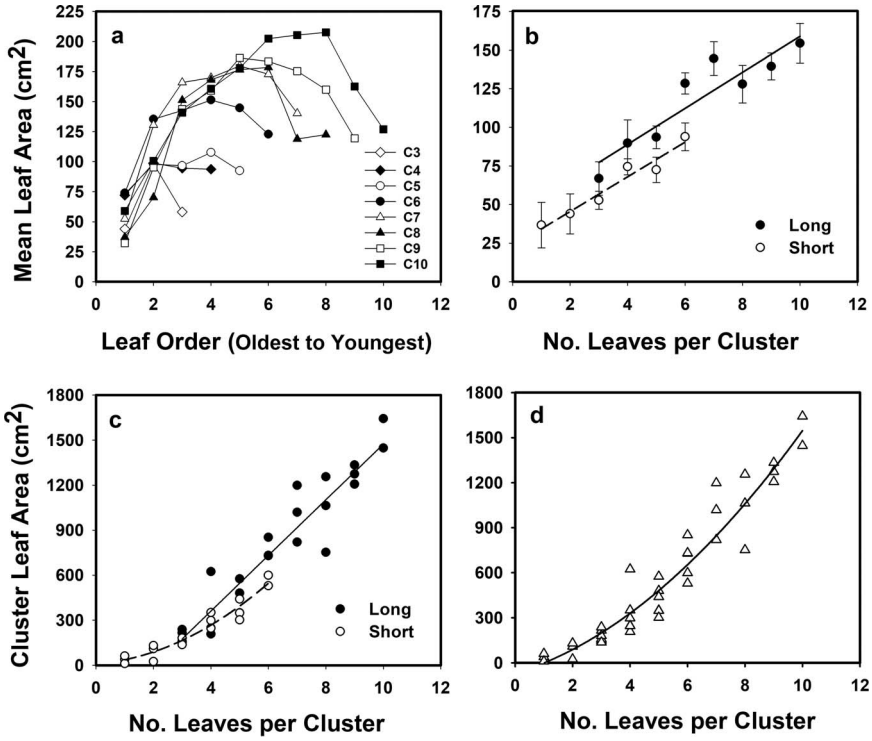

FIG. 3. Results for several analyses of measured cluster leaf areas. (a) Mean leaf area per leaf position (oldest to youngest) for eight long cluster sizes ranging from 3 (C3) to 10 (C10) leaves per cluster ($N = 2$–4 leaves per position per cluster size); (b) mean (± 1 SD) leaf area plotted against cluster size separately for long and short clusters; (c) total cluster leaf area *versus* the number of leaves in short ($N = 17$) and long ($N = 24$) clusters; and (d) total cluster leaf area *versus* the number of leaves in combined clusters ($N = 41$). Quadratic curve fits ($Y = aX + bX^2 + Y_0$) were stronger than linear regressions ($Y = aX + Y_0$) for short clusters in panel c and for combined cluster sizes in panel d.

Table 2. Descriptive statistics for measured area of individual leaves and total leaf area for entire leaf clusters, calculated for long and short clusters separately and then for long and short clusters combined, plus estimated total leaf area of ramets in different main-stem length classes.

	N	Mean	Maximum	Minimum	SD	CV (%)
Leaf (cm^2)						
Long clusters	155	126.5	232.0	6.1	53.9	42.6
Short clusters	57	69.4	130.6	4.0	31.1	44.8
Combined clusters	212	111.2	232.0	4.0	54.9	49.4
Leaf cluster (cm^2)						
Long clusters	24	817.0	1,642.1	148.4	446.5	54.6
Short clusters	17	232.8	598.2	10.2	177.4	76.2
Combined clusters	41	574.8	1,642.1	10.2	460.5	80.1
Ramet (m^2)						
0.00–0.49 m	10	0.093	0.102	0.063	0.015	15.8
0.50–0.99 m	10	0.158	0.261	0.101	0.048	30.6
1.00–1.49 m	9	0.583	0.878	0.336	0.182	31.1
1.50–1.99 m	9	1.066	1.527	0.596	0.341	32.0
2.00–2.50 m	10	1.662	2.883	0.687	0.696	41.9
All lengths	48	0.708	2.883	0.063	0.696	98.4

differed even more (3.5-fold) between the cluster types (Mann-Whitney $U = 46.0$, $P < 0.001$).

Total cluster leaf area was significantly correlated with the number of leaves per cluster, as expected (Table 1, Fig. 3c, d). The strength of this relationship was similar for just long clusters, just short clusters, and for combined clusters. The best fit for short clusters was quadratic, whereas the linear and quadratic fits for long clusters were nearly identical.

Estimated total ramet leaf area averaged 0.71 m^2, with a median of 0.55 m^2 and an overall range of 0.06–2.88 m^2 ($N = 48$, Table 2), The means across the five ramet size categories showed a nearly 18-fold range, whereas maximums showed a 28-fold range. Total ramet leaf area was exponentially related to main-stem length (Table 1, Fig. 1e). Variation around the fitted curve appeared to increase with ramet size, which was confirmed by the rise in both SD and CV values

Table 3. Ramet density and foliar descriptive statistics calculated across the 2×2 m quadrats within each of the eight patch transects (coded A1–C10) plus one-way ANOVA test results. The overall ANOVA significance value was $P = 0.008$ for LAD and $P < 0.001$ for all other variables. Abbreviations: LAI = leaf area index, LAD = leaf area density, n.s.d. = no significant difference.

Variable	A1	B8	B9	C1	C2	C3	C7	C10	All quadrats	ANOVA pairwise results
No. quadrats	9	8	12	7	5	6	7	4	58	
No. *Asimina* stems										
Mean	16.2	18.9	26.6	6.7	9.0	9.5	13.3	15.0	15.8	B9 > B8, B8 > all others, A1 > C1
SD	4.4	6.3	5.5	3.6	5.5	3.9	4.5	2.9	8.1	
Maximum foliage height (m)										
Mean	0.83	1.21	1.88	1.57	1.29	1.62	1.28	1.03	1.38	B9 > B8 = C10 = A1, all others n.s.d.
SD	0.30	0.35	0.54	0.47	0.34	0.36	0.47	0.07	0.53	
Minimum foliage height (m)										
Mean	0.21	0.20	0.30	0.51	0.32	0.40	0.22	0.26	0.30	C1 > A1 = B8, all others n.s.d.
SD	0.05	0.07	0.12	0.17	0.14	0.13	0.06	0.08	0.14	
Canopy depth (m)										
Mean	0.61	1.01	1.58	1.06	0.97	1.22	1.07	0.77	1.08	B9 > B8 = C10 = A1, all others n.s.d.
SD	0.30	0.36	0.58	0.60	0.32	0.43	0.43	0.13	0.52	
No. leaf clusters										
Mean	32.2	86.5	97.9	37.7	51.2	51.2	60.9	50.5	62.3	B9 > C1 = A1, all others n.s.d.
SD	11.1	48.9	26.2	13.6	28.9	27.6	40.3	15.2	37.0	
LAI ($m^2\ m^{-2}$)										
Mean	0.42	1.13	1.28	0.49	0.67	0.67	0.80	0.66	0.81	B9 > C1 = A1, all others n.s.d.
SD	0.15	0.64	0.34	0.18	0.38	0.36	0.53	0.20	0.48	
LAD ($m^2\ m^{-3}$)										
Mean	0.81	1.12	0.87	0.53	0.67	0.53	0.72	0.86	0.78	n.s.d.
SD	0.36	0.58	0.27	0.14	0.24	0.13	0.22	0.15	0.35	

across the five size categories (Table 2). However, total ramet leaf area was linearly and very strongly correlated with the total number of leaves (R^2 = 0.97, Table 1), and the relationship was slightly stronger for a $\log_{10}$–$\log_{10}$ plot of the same variables ($R^2 = 0.99$; data not shown).

Patch Foliar Structure. The eight patches showed wide variation in foliar structure on the basis of their 2-m-wide belt transects (Table 3). All seven variables differed significantly among patches ($P = 0.008$ for LAD, $P < 0.001$ for all others). Means per 2 × 2 m quadrat differed by over twofold for maximum height, minimum height, canopy depth, and estimated LAD, by threefold for the number of leaf clusters and estimated LAI, and by nearly fourfold for *A. triloba* stem density. Considerable within-patch spatial variation was observed in the field for most patches and confirmed quantitatively by the relatively high standard deviations for many variables.

Patch B9 was the largest in terms of both transect length and total areal coverage. Pairwise tests showed that it also had significantly greater ramet density, height, and denser foliage (more clusters, greater canopy depth, higher LAI and LAD), whereas patches A1 and C1 had significantly lower stem and foliar densities (Table 3). LAI and LAD showed some important contrasts. There were a few pairwise patch differences for LAI, but none for LAD, and the rank orders among patch means were quite different. For both variables, B8 and B9 were among the top three and C1 and C3 were among the bottom three, but the ranks shifted substantially for the remaining patches. LAI and canopy depth were significantly and positively related (linear, $P = 0.050$), but with a modest correlation ($R^2 = 0.50$). Nonparallel variation in their relationship produced the divergent ranking patterns of LAI and LAD across patches.

Foliar variable means plotted against patch size (transect length) mostly showed substantial scattering with no obvious visual trends and with nonsignificant regressions ($P = 0.16$–0.70, $R^2 = 0.07$–0.30; data not shown). A notable exception is that ramet density was positively correlated with patch size (linear: $P = 0.037$, $R^2 = 0.54$, slope = 0.930). Patches C1 (higher density than predicted) and C10 (lower than predicted) showed the greatest deviations from the regression line and lowered the strength of the correlation (data not shown).

Discussion. Ramet Architecture and Leaf Area. There are few published data on *A. triloba* architecture and no data on total ramet leaf area with which the results of this study can be compared. The extensive research on *A. triloba* ramet demography and growth by Hosaka *et al.* (2005, 2008, 2016) did not include stem length or leaf area measurements. Young (1985) quantified architectural variables not measured here, including branch dimensions, bifurcation ratios, leaf size/mass relationships, and laminar orientations. Young also reported individual leaf areas by position within clusters but did not measure or estimate total leaf area at the ramet level, and the measured ramets did not have any second- or third-order foliage. Summing the mean leaf areas listed by Young for successive leaf positions within five-leaf primary clusters yields a total of 606 cm^2. This is lower than the long-cluster leaf area of 817 cm^2 reported here (Table 2), but the latter value includes clusters ranging from 3 to 10 leaves, with an average (6.5) greater than the mean of 5.4 leaves per cluster in Young's study.

Young and Yavitt (1987) measured individual leaf areas by location along primary branches in the same study site used by Young (1985), but also did not quantify total ramet leaf area. Both Young (1985) and Young and Yavitt (1987) found that mean leaf size increased from the proximal (oldest) to distal (youngest) leaves within long clusters, consistent with the pattern demonstrated here. However, the leaf areas they reported are somewhat lower (range 32–132 cm^2) than most of the values measured at AMW (Table 2, Fig. 3a).

The visual impression that *A. triloba* shoot organization is well regulated is supported by the highly significant relationships among all ramet and leaf-cluster variables documented in this study, most of which had strong correlations as well. However, the foliar structure of *A. triloba* ramets varies at several levels (leaf, cluster, ramet). Mean leaf area by position within clusters, mean leaf areas across clusters of different size, numbers of leaves per cluster, and total cluster leaf area all differ between long and short clusters. In addition, the numbers of long and short clusters and the ratio between them differ among ramets. The exponential regressions for the number of clusters or the number of leaves *versus* main-stem length were highly significant ($P < 0.0001$), but the amount of variation explained by the regressions was lower

than for other pairs of architectural variables ($R^2 =$ 0.55–0.74; Table 1).

The strongest foliar correlations were (a) total cluster leaf area *versus* number of leaves per cluster (linear: $R^2 = 0.90$–0.94), (b) total number of leaves *versus* total number of clusters per ramet (linear: $R^2 = 0.98$), and (c) total leaf area *versus* total number of leaves per ramet (linear: $R^2 = 0.97$, $\log_{10}$-$\log_{10}$ linear: $R^2 = 0.99$). These relationships suggest dynamic physiological and developmental integration among the number and type of clusters on a ramet, how many leaves are in each cluster, and the sizes of those leaves in a way that produces a very high correlation between total number of leaves and total leaf area per ramet. If so, this result may be similar to the strong "dynamic scaling" relationship documented for a nonclonal forest herb (Koyama *et al*. 2012). The high numbers of clusters (up to 65) and leaves (up to 299) on larger *A. triloba* ramets would offer numerous adjustment locations for leaf number and size dispersed across the shoot. Once a long or short cluster has been initiated and persists across years, the number of leaves and their fully expanded sizes could be adjusted within each cluster in response to (a) overall environmental conditions, such as spring temperature and precipitation; (b) spatially or temporally variable light environments across the ramet's canopy; and (c) carbohydrates and nutrients available for allocation to leaves, resources that were either stored over winter or acquired during the current growing season. This is consistent with the demonstration of Young and Yavitt (1987) that numerous ecophysiologically important leaf variables differ substantially within long clusters for leaves that expand before *versus* after spring canopy closure. The hypothesis about dynamic adjustment at the cluster or ramet level could be tested through multiyear studies of environmental conditions and leaf production by marked clusters within and across different ramets.

CLUSTER-GROUP LEAF-AREA ESTIMATION. A preliminary indication of the accuracy of the cluster-group leaf-area scaling method can be achieved through limited random subsampling from the pool of 41 cluster leaf areas without constraining whether they are long or short clusters. The cluster areas in a subsample can be summed and compared with the total area estimated using the weighted cluster-group scaling factor. This was done once each for 4, 8, 12, 16, and 20 clusters. The corresponding results for measured *versus* estimated total leaf areas (m^2) are as follows (% error in parentheses): 0.191 *versus* 0.209 (9.1%), 0.528 *versus* 0.418 (20.8%), 0.567 *versus* 0.628 (10.7%), 0.899 *versus* 0.837 (6.9%), and 1.073 *versus* 1.046 (2.5%). There is no consistent trend with cluster size in terms of over- or underestimating the actual area. The average percent error across the cluster sizes of 2.1% is encouraging but should be interpreted with caution because of the repeated random sampling from the same pool, with subsamples representing up to half the total pool size.

Several facts together suggest that total leaf area estimates based on cluster counting in even fairly small plots (*e.g*., the 2 × 2 m quadrats in this study) should not generate large errors for patches in the AMW study site. These facts include (a) the strong correlations between cluster size and cluster total leaf area, (b) the double weighting of the cluster-group multiplier to include the proportions of long and short cluster sizes across ramets and the mean leaf areas of individual cluster sizes, (c) the similarity between the long:short cluster ratio in the cluster leaf area sample (24:17, 59%:41%) and the ratio recorded across the 48 ramets (378:231, 61%:39%), (d) the modest overall estimation error suggested by the random subsampling results above, and (e) the cluster densities recorded in transects during patch sampling. With respect to the latter point, cluster counts in the 58 2 × 2 m patch sampling quadrats across the eight patches showed that 93% had more than 20 clusters and 47% had more than 50 (mean = 62.3, median = 49, range 13–153). The greater the cluster count, the lower the likelihood that individual clusters can cause the weighted multiplier to markedly over- or underestimate the actual total leaf area.

The validity of this method needs to be tested in future research by comparing total leaf areas measured independently on cluster groups extracted from sample plots in the field *versus* cluster-scaled estimates for those plots. The method appears to work for patches under undisturbed canopy in the AMW study site, but it should be considered preliminary and site specific until demonstrated otherwise.

PATCH LAI AND OVERALL STRUCTURE. The few studies reporting data on *A. triloba* patch structure vary widely in their purposes, site conditions, ramet size, and in understory dominance by the *A. triloba* canopy, and there are no published

measurements of *A. triloba* LAI. Individual 2 × 2 m quadrat LAI estimates in this study ranged from 0.17 to 2.00 m^2 m^{-2}, and mean patch LAI values spanned 0.42–1.28 m^2 m^{-2}, with a grand mean across patches of 0.77 m^2 m^{-2}. These values are comparable with those reported for understory tree saplings by Poorter and Werger (1999; 0.53–0.88 m^2 m^{-2}) in lowland Amazonia and by Chianucci et al. (2014; 0.5–2.4 m^2 m^{-2}) in Italy but are considerably lower than the 4.0–6.6 m^2 m^{-2} documented by Beckage et al. (2008) for *Rhododendron maximum* L. in western North Carolina, USA. More broadly, LAI values at AMW are in the lower 40% of the range of understory whole-community LAI (0.0–3.0 m^2 m^{-2}) calculated by Liu et al. (2017) across the world's forests using remote sensing.

Asimina triloba patch structure is heterogenous, even for the smaller patches in our study that could be single genets. They often do not show an idealized symmetrical, domelike shape with taller, older, and denser ramets toward the center and shorter, younger, less dense ramets on the margins, a shape that might be expected under steady patch expansion and continual internal ramet growth after genet establishment in a fairly homogeneous environment. Mean ramet density did increase significantly with patch size, which would be expected if patch footprint is generally correlated with age and new ramet production inside patches is at least as common as ramet initiation on the patch margins, a pattern documented by Hosaka *et al*. (2005). However, no other foliar variable, including LAI, showed a significant relationship with patch size, so spatially variable or unpredictable factors—such as multiple genet intermixing, species-specific overstory composition and light transmission, understory composition and competition, belowground competition, ramet damage/resprouting, and ramet mortality—either (a) reduce the likelihood of patches developing predictable ramet densities and profile symmetry or (b) degrade a patch's earlier symmetry over time. The high degree of heterogeneity within patches thus eliminates the possibility of using a whole-patch model of ramet and foliar development to estimate LAI consistently at this higher structural scale. More intensive sampling at smaller scales within patches is required to understand patch effects on light transmission, and this reinforces the usefulness of the fairly rapid cluster-group scaling method developed here.

Asimina triloba can play an important role in the understory across a range of physiographic conditions, forest stand ages and compositions, and disturbance regimes. The leaf-area and LAI scaling methods developed here are probably most applicable to undisturbed upland sites with generally low understory light levels and moderate soil resources, where *A. triloba* is less likely to grow into tree-sized individuals that can dominate the understory more completely across large areas. In more massive *A. triloba* stands, canopy depth, leaf cluster density, and LAI would depend as usual on light attenuation by the overstory. Internal competition would play an increasing role as it thins ramet density, raises the minimum foliar height, and alters the relationships between foliar structure and main-stem length. It is possible that the cluster-group scaling method for estimating LAI would still work, but it would become more difficult to determine cluster inclusion within a defined plot as average *A. triloba* height increases. Ramet growth rates and architectures would also be expected to differ under or near canopy gaps as compared with the full understory, so LAI estimation on the basis of cluster counts would also have to be quantified across a broader gap–understory gradient. Extrapolating the approach to other shrub taxa is worth exploring, although the method may not work as well for species in which branching architecture and foliar displays are either more complicated or more phenotypically variable than *A. triloba*.

Conclusions. With reference to the original questions of this study, we can conclude the following for *Asimina triloba*: (a) ramet foliar structure shows highly significant and strong relationships across leaf, leaf cluster, and ramet levels; (b) total leaf area and LAI of an *A. triloba* patch can be determined nondestructively by systematically sampling portions of the patch and applying a weighted cluster-based scaling factor to groups of clusters sampled independently without reference to their association with specific ramets; and (c) patches below undisturbed canopy vary substantially in numerous foliar variables, including LAI, but they are spatially heterogeneous and their foliar organization shows little predictability overall as a function of patch size. The cluster-based foliar scaling strategy for *A. triloba* developed here is particularly important for such heterogeneous patches, and may be applicable in

other undisturbed mature upland forests. However, it would need to be calibrated on a site-specific basis across a wider range of physiography, canopy disturbance conditions, and patch statures.

Literature Cited

AUGSPURGER, C. K., J. M. CHEESEMAN, AND C. F. SALK. 2005. Light gains and physiological capacity of understorey woody plants during phenological avoidance of canopy shade. Functional Ecology 19: 537–546.

BAUMER, M. AND J. R. RUNKLE. 2010. Tree seedling establishment under the native shrub, *Asimina triloba*. Castanea 75: 421–432

BECKAGE, B., B. D. KLOEPPEL, J. A. YEAKLEY, S. F. TAYLOR, AND D. C. COLEMAN. 2008. Differential effects of understory and overstory gaps on tree regeneration. Journal of the Torrey Botanical Society 135: 1–11.

BOTKINS, J., K. W. POMPER, J. D. LOWE, AND S. B. CRABTREE. 2012. Pawpaw patch genetic diversity, and clonality, and its impact on the establishment of invasive species in the forest understory. Journal of the Kentucky Academy of Science 73: 113–121.

CHIANUCCI, F., A. CUTINI, P. CORONA, AND N. PULETTI. 2014. Estimation of leaf area index in understory deciduous trees using digital photography. Agricultural and Forest Meteorology 198–199: 259–264.

FASSNACHT, K. S., S. T. GOWER, J. M. NORMAN, AND R. E. MCMURTRIE. 1994. A comparison of optical and direct methods for estimating foliage surface area index in forests. Agricultural and Forest Meteorology 71: 183–207.

GOODRICH, K. R., L. A. ORTIZ, AND D. J. COUGHLIN. 2016. Unusual twig "twistiness" in pawpaw (*Asimina triloba*) provides biomechanical protection for distal foliage in high winds. American Journal of Botany 103: 1872–1879.

HOSAKA, N., S. GOMEZ, N. KACHI, J. F. STUEFER, AND D. F. WHIGHAM. 2005. The ecological significance of clonal growth in the understory tree, pawpaw (*Asimina triloba*). Northeastern Naturalist 12: 11–22.

HOSAKA, N., N. KACHI, H. KUDOH, J. F. STUEFER, AND D. F. WHIGHAM. 2008. Patch structure and ramet demography of the clonal tree, *Asimina triloba*, under gap and closed-canopy. Plant Ecology 197: 219–228.

HOSAKA, N., N. KACHI, H. KUDOH, J. F. STUEFER, AND D. F. WHIGHAM. 2016. Compensatory growth of the clonal understory tree, *Asimina triloba*, in response to small-scale disturbances. Plant Ecology 217: 471–480.

IWABE, R., K. KOYAMA, AND R. KOMAMURA. 2021. Shade avoidance and light foraging of a clonal woody species, *Pachysandra terminalis*. Plants 10: 809. https://doi.org/10.3.390/plants10040809.

JACQUART, E. M., T. V. ARMENTANO, AND A. L. SPINGARN. 1992. Spatial and temporal tree responses to water stress in an old-growth deciduous forest. American Midland Naturalist 127: 158–171.

KAWAMURA, K. AND H. TAKEDA. 2002. Light environment and crown architecture of two temperate *Vaccinium* species: Inherent growth rules versus degree of plasticity in light response. Canadian Journal of Botany 80: 1063–1077.

KAWAMURA, K. AND H. TAKEDA. 2004. Rules of crown development in the clonal shrub *Vaccinium hirtum* in a low-light understory: A quantitative analysis of architecture. Canadian Journal of Botany 82: 329–339.

KEMPF, J. S. AND S. T. A. PICKETT. 1981. The role of branch length and angle in branching patterns along a successional gradient. New Phytologist 88: 111–116.

KOYAMA, K., Y. HIDAKA, AND M. USHIO. 2012. Dynamic scaling in the growth of a non-branching plant, *Cardiocrinum cordatum*. PLOS One 7(9): e45217.

KÜPPERS, M. 1989. Ecological significance of above-ground architectural patterns in woody plants: A question of cost–benefit relationships. Trends in Ecology and Evolution 4: 375–379.

LAGRANGE, R. L. AND E. J. TRAMER. 1985. Geographic variation in size and reproductive success in the paw paw (*Asimina triloba*). Ohio Journal of Science 85: 40–45.

LAURANS, M. AND G. VINCENT. 2016. Are inter- and intraspecific variations of sapling crown traits consistent with a strategy promoting light capture in tropical moist forest? Annals of Botany 118: 983–996.

LINDSEY, A. A., D. V. SCHMELZ, AND S. A. NICHOLS. 1969. Natural areas in Indiana and their preservation. Indiana Natural Areas Survey, Purdue University, Lafayette, IN, 594 pp.

LIU, Y., R. LIU, J. PISEK, AND J. M. CHEN. 2017. Separating overstory and understory leaf area indices for global needleleaf and deciduous broadleaved forests by fusion of MODIS and MISR data. Biogeosciences 14: 1093–1110

LUKEN, J. O., L. M. KUDDES, T. C. THOLEMEIER, AND D. M. HALLER. 1997. Comparative responses of *Lonicera maackii* (Amur honeysuckle) and *Lindera benzoin* (spicebush) to increased light. American Midland Naturalist 138: 331–343.

MCGARVEY, J. C., N. A. BOURG, J. R. THOMPSON, W. J. MCSHEA, AND X. SHEN. 2013. Effects of twenty years of deer exclusion on woody vegetation at three life-history stages in a mid-Atlantic temperate deciduous forest. Northeastern Naturalist 20: 451–468.

MERCADER, R. J., T. J. PAULSON, P. J. ENGLEKEN, AND L. R. APPENFELLER. 2020. Defoliation by a native herbivore, *Omphalocera munroei*, leads to patch size reduction of a native plant species, *Asimina triloba*, following small-scale removal of the invasive shrub, Amur honeysuckle, *Lonicera maackii*. Plant Ecology 221: 125–139.

NASH, L. J. AND W. R. GRAVES. 1993. Drought and flood stress effects on plant development and leaf water relations of five taxa of trees native to bottomland hardwoods. Journal of the American Society of Horticultural Science 118: 845–850.

NICOLA, A. AND S. T. A. PICKETT. 1983. The adaptive architecture of shrub canopies: Leaf display and biomass allocation in relation to light environment. New Phytologist 93: 301–310.

PARKER, G. R. 1989. Old-growth forests of the central hardwood region. Natural Areas Journal 9: 5–11.

PEARCY, R. W. AND W. YANG. 1996. A three-dimensional crown architecture model for assessment of light capture and carbon gain by understory plants. Oecologia 108: 1–12.

Pearcy, R. W., H. Muraoka, and F. Valladares. 2005. Crown architecture in sun and shade environments: Assessing function and trade-offs with a three-dimensional simulation model. New Phytologist 166: 791–800.

Petty, R. 1964. Forest analysis of a mesic ravine, Parke County, Indiana. Proceedings of the Indiana Academy of Science 74: 308–313.

Petty, R. O., E. C. Williams, Jr., and R. A. Laubengayer. 1961. Ecological studies of a ridge forest and adjacent flood plain, Parke County, Indiana. Final Report, Atomic Energy Commission Contract AT(11-1)-547. Wabash College, Crawfordsville, Indiana, 197 pp.

Pickett, S. T. A. and J. S. Kempf. 1980. Branching patterns in forest shrubs and understory trees in relation to habitat. New Phytologist 86: 219–228.

Poorter, L. and M. J. A. Werger. 1999. Light environment, sapling architecture, and leaf display in six rain forest tree species. American Journal of Botany 86:1461–1473.

Sipe, T. W. and R. J. Yamulla. 2021. Compositional dynamics and light regimes in a midwestern old-growth forest preserve. Journal of the Torrey Botanical Society 148: 223–242.

Slater, M. A. and R. C. Anderson. 2014. Intensive selective deer browsing favors success of *Asimina triloba* (paw paw) a native tree species. Natural Areas Journal 34: 178–187.

Sterck, F. J., R. A. Duursma, R. W. Pearcy, F. Valladares, M. Cieslak, and M. Weemstra. 2013. Plasticity influencing the light compensation point offsets the specialization for light niches across shrub species in a tropical forest understorey. Journal of Ecology 101: 971–980.

Valladares, F., S. J. Wright, E. Lasso, K. Kitajima, and R. W. Pearcy. 2000. Plastic phenotypic response to light of 16 congeneric shrubs from a Panamanian rainforest. Ecology 81: 1925–1936.

Wang, J., T. Xu, Y. Wang, G. Li, I. Abdullah, Z. Zhong, J. Liu, W. Zhu, L. Wang, D. Wang, and F. Yu. 2020. A meta-analysis of effects of physiological integration in clonal plants under homogeneous vs. heterogeneous environments. Functional Ecology 35: 578–589.

Weiss, M., F. Baret, G. J. Smith, I. Jonckheere, and P. Coppin. 2004. Review of methods for in situ leaf area index (LAI) determination Part II. Estimation of LAI, errors, and sampling. Agricultural and Forest Meteorology 121: 37–53.

Willson, M. F. and D. W. Schemske. 1980. Pollinator limitation, fruit production, and floral display in pawpaw (*Asimina triloba*). Bulletin of the Torrey Botanical Club 107: 401–408.

Young, D. R. 1985. Crown architecture, light interception, and stomatal conductance patterns for sympatric deciduous and evergreen species in a forest understory. Canadian Journal of Botany 63: 2425–2429.

Young, D. R. 1987. Daily and seasonal variations in the water relations of the understory tree, *Asimina triloba*. Oecologia Plantarum 8: 59–68.

Young, D. R. and J. B. Yavitt. 1987. Differences in leaf structure, chlorophyll, and nutrients for the understory tree *Asimina triloba*. American Journal of Botany 74: 1487–1491.